Supplementary Materials associated with:

Principles of dimer-specific gene regulation revealed by a comprehensive characterization of NF-κB family DNA binding

Trevor Siggers[1,7], Abraham B Chang[2,7], Ana Teixeira[3], Daniel Wong[3], Kevin J Williams[2], Bilal Ahmed[1,4], Jiannis Ragoussis[3], Irina A Udalova[5], Stephen T Smale[2] & Martha L Bulyk[1,4,6,*]

[1]Division of Genetics, Department of Medicine, Brigham & Women's Hospital and Harvard Medical School, Boston, Massachusetts, USA. [2]Molecular Biology Institute and Department of Microbiology, Immunology, and Molecular Genetics, University of California Los Angeles, Los Angeles, CA, USA. [3]Wellcome Trust Centre for Human Genetics, Oxford University, Oxford, UK. [4]Harvard-MIT Division of Health Sciences and Technology, Harvard Medical School, Boston, Massachusetts, USA. [5]Kennedy Institute of Rheumatology, Imperial College, London, UK. [6]Department of Pathology, Brigham & Women's Hospital and Harvard Medical School, Boston, Massachusetts, USA.

[7]These authors contributed equally to this work.

[*]Correspondence should be addressed to M.L.B. (mlbulyk@receptor.med.harvard.edu).

Nature Immunology doi:10.1038/ni.2151

Supplementary Discussion

Specificity of RelB:p52 heterodimer binding

It has been reported that RelB:p52, but not RelB:p50 and RelA:p50, can bind well to the murine BLC-kB site (mBLC: 5'-GGGAGATTTG-3'), a non-traditional κB site sequence[1]. RelB:p52 is the primary NF-κB dimer activated in response to the alternative NF-κB pathway[2,3]. More recently, it was reported that RelB:p52 is less discriminatory than RelA:p50 and can bind to a broader set of κB site sequences[4]. Binding sites unique to RelB:p52 would provide a mechanism for the cell to differentiate target genes of the alternative NF-κB pathway from those of the classical pathway activating RelA:p50[5].

However, contradictory reports suggest that full-length RelB:p52 and RelA:p50 do not bind to murine BLC-κB, but can bind weakly and with similar affinities to the human BLC-κB site (hBLC: 5'-GGGGGCTTTT-3'), compared with robust binding of each dimer to a control κB site (con_κB: 5'-GGGACTTTCC-3')[6]. Our PBM data exhibit the same relative preferences for RelB:p52(H): mBLC (z-score=0.7, i.e., no significant binding), hBLC (z-score=4.0, i.e., moderate binding), con_κB (z-score=11.1, i.e., strong binding). Furthermore, we observe these same relative preferences for RelB:p50(H) (z-scores: 0.9, 3.1, 8.5, respectively) and RelA:p50(H) (z-scores: 0.7, 4.3, 13.8, respectively).

Our data support the finding that RelB:p52 and RelB:p50 do not differ significantly in their DNA binding preferences. Furthermore, we now extend this to include all NF-κB heterodimers, demonstrating that NF-κB heterodimers exhibit common binding preferences to the ~3,300 κB site sequences examined in this study. Modest binding differences that have been reported for heterodimers[4], may be below the resolution of our approach and may prove functionally important *in vivo* and will need to be examined in greater depth in the future. However, the common binding preferences presented in this work and others[6] suggest that the regulation of distinct sets of genes by different heterodimers is likely to be achieved primarily through alternative mechanisms, such as dimer-specific interactions with co-regulatory proteins[7], dimer-specific synergy with other transcription factors, or dimer-specific conformational differences[4,8,9].

`

Supplementary Methods

Scoring 10-mers using universal PBM (uPBM) data. Scores for 10-mers (e.g., 10-bp κB sites) were determined using the 8-mer and 7-mer data available from uPBM experiments. The method is based on two assumptions: (1) log of the k-mer median fluorescence intensity is proportional to the equilibrium binding energy of the protein to that sequence, and (2) binding energy for a k-mer can be partitioned into the binding energy to each individual base. K-mers are scored by adding up the ln(F) values (i.e., the binding energies) for constituent shorter k-mers taking care not to double-count the contribution from any base position. For example, we can score a 9-mer by adding the ln(F) values for the two constituent 8-mers and subtracting the ln(F) value for the 7-mer so as not to double-count contributions form the central 7-mer (**Supplementary Fig. 8a**). K-mers can be scoring using *contiguous* or *gapped* constituent k-mers (**Supplementary Fig. 8b and 8c**), all of which are measured in a uPBM experiment. In this work, 10-bp κB sequences were scored using contiguous and gapped 8-mers following three simple scoring scheme/patterns (**Supplementary Fig. 9**), final scores were an average of the three separate scores. We found no significant difference when final scores were average over more scoring schemes (data not shown).

Position weight matrix (PWM) scoring. To score binding site sequences using the PWMs we used the following formalism.

$$p_{i,j} = \frac{(f_{i,j} + sb_i)}{(\sum_i f_{i,j} + s)} \qquad (1)$$

PWM probability of an A,C,G or T (i=0,1,2,3 respectively) occurring at position j of the k-mer (i.e., sequence) being evaluated.

$f_{i,j}$: Count frequency defining the position frequency matrix, as provided in JASPAR

b_i : Nucleotide background frequencies: 0.28 (A,T); 0.22 (C,G)

`

s: Pseudo-count to deal with zeros (s = 0.001)

$$S_{i,j} = \log_2\left(\frac{p_{i,j}}{b_i}\right) \qquad (2)$$

Scoring matrix used to score k-mers. PWM score is the sum over all positions (j) of the corresponding $S_{i,j}$ values for a particular k-mer.

PWMs cutoffs are defined in terms of the score distribution of true positive k-mers. True positive k-mers are those whose distribution is defined by the PWM probability matrix ($p_{i,j}$). Score cutoff values are expressed in terms of the standard deviation (σ) from the expected PWM score (ES) for a true (or positive) k-mer.

$$ES = \sum_j \sum_i p_{i,j} S_{i,j} \qquad (3)$$

$$\sigma^2 = \sum_j \sum_i p_{i,j} S_{i,j}^2 - \sum_j (\sum_i p_{i,j} S_{i,j})^2 \qquad (4)$$

We refer to PWM cutoffs as either 1 standard deviation (SD) below ES (i.e., 1 SD = ES – sqrt(σ^2)), or 2 SDs below ES (i.e., 2 SD = ES – 2*sqrt(σ^2)) which is a much more liberal cutoff for the PWM (i.e., more sequences will score above this cutoff).

Determining Traditional vs. Non-traditional κB sites. Non-traditional κB sites were defined as those that score poorly by all four NF-κB position weight matrices (PWMs) in JASPAR database[10]: NFkB (MA0061)[11]; c-Rel (MA0101)[12]; p50:p50 (MA0105)[12]; p65:p65 (MA0107)[12]. The PWM scoring function used is as described above. Non-traditional sites defined at the 1 SD cutoff level (see section above 'Position weight matrix (PWM) scoring') must score below the 1 SD threshold for *all four* JASPAR PWMs. If the k-mer is longer than the PWM the score from the highest scoring sub-sequence is used. PWM cutoff values for the four matrices are: NFkB (MA0061, 1 SD =10.9, 2 SD=8.2), cRel (MA0101, 1 SD=7.6, 2 SD=4.5), p50:p50 (MA0105, 1 SD =14.0, 2 SD=11.4), p65:p65 (MA0107, 1 SD=12.9, 2 SD=10.9).

Generating 12-bp κB dataset. We constructed a linear model to score 12-bp sites using our 10-bp kB site PBM data and correction terms determined by linear regression (see

`

Supplementary Fig. 10 for schematic). We measured the effect on binding of all 4^2 = 16 possible pairs of flanking sequences (M,N) on 22 distinct 10-bp kB sites (i.e., the 16 12-bp sites MXXXXXXXXXXN (M,N = any base), based on each 10-bp site XXXXXXXXXX). Fluorescence values for the 12-bp κB sites was transformed to a z-score using the mean and standard deviation defined by the ~3,300 10-bp κB site measurements. Binding differences occurred only with the addition of a Gua base to either 5′, and the effect was dependent on the G-content of adjacent bases. We determined five regression features (see **Supplementary Fig. 10a**) and for each NF-κB dimer PBM experiment we performed a linear regression analysis on the 16x22 = 352 binding measurements to determine the weights of the five features. Note that for all PBM experiments the array contained all 352 12-bp probes as well as our full complement of 10-bp probes. The calculated weights were used to calculate the z-scores for the sixteen 12-bp sites generated from each 10-bp kB site in our dataset (see **Supplementary Fig. 10b,c** for scoring scheme; see **Supplementary Fig. 11** for demonstration of prediction accuracy, i.e., predicted 12-bp z-scores versus measured 12-bp z-scores).

Enrichment of κB sites in ChIP positive regions. Three chromatin immunoprecipitation (ChIP) datasets were analyzed in this work:

(1) RelA/p65 binding in lipopolysaccharide (LPS)-stimulated human monocytes[13]: 489 high significance PET3 clusters, determined by ChIP-PET, were used as 'bound' regions (downloadable as supplementary data file from Young lab website). Length-matched genomic regions from either side of each 'bound' region (separated by a 500-bp spacer) were used as representative 'unbound' genomic regions. Length-matching was performed using only non-repeat sequence as provided by UCSC genome repository.

(2) RelA/p65 binding in TNF-stimulated human lymphoblastoid cell lines[14]. 15,516 high significance regions determined by ChIP-seq (downloadable as supplementary data file) were used as 'bound' regions. Length-matched genomic regions from either side of each 'bound' region (separated by a 500-bp spacer) were used as representative 'unbound' genomic regions. Length-matching was

`

performed using only non-repeat sequence as provided by UCSC genome repository.

(3) Binding of all five NF-κB in LPS-stimulated U937 cells[15]. 8,906 human promoter regions were analyzed by ChIP-chip. High significance regions (as reported in Figure 1[15], enrichment p-value < 0.002) were used as 'bound' regions. Low significance regions (p-value > 0.5) were used as 'unbound' regions.

Genomic regions (foreground/bound and background/unbound) were scored according to the top-scoring PBM-determined κB sites identified within each region. For this work 12-bp κB sites were used (see section above 'Generating 12-bp kB dataset' for more details). All genomic searches were performed explicitly with k-mer data, and not PWMs, using custom Perl scripts. Receiver-operating-characteristic (ROC) curve analyses were performed to quantify whether bound regions scored more highly than the unbound regions. Area under the ROC curve (AUC) values are reported to quantify the enrichment, and a Wilcox-Mann-Whitney (WMW) U test was applied to calculate the significance of each AUC value. AUC and WMW U test values were calculated in the R statistical package using the wilcox.test function.

Supplementary References

1. Bonizzi, G. *et al.* Activation of IKKalpha target genes depends on recognition of specific kappaB binding sites by RelB:p52 dimers. *EMBO J* 23, 4202-4210 (2004).
2. Senftleben, U., Li, Z.W., Baud, V. & Karin, M. IKKbeta is essential for protecting T cells from TNFalpha-induced apoptosis. *Immunity* 14, 217-230 (2001).
3. Xiao, G., Harhaj, E.W. & Sun, S.C. NF-kappaB-inducing kinase regulates the processing of NF-kappaB2 p100. *Mol Cell* 7, 401-409 (2001).
4. Fusco, A.J. *et al.* NF-kappaB p52:RelB heterodimer recognizes two classes of kappaB sites with two distinct modes. *EMBO Rep* 10, 152-159 (2009).
5. Hoffmann, A., Natoli, G. & Ghosh, G. Transcriptional regulation via the NF-kappaB signaling module. *Oncogene* 25, 6706-6716 (2006).
6. Britanova, L.V., Makeev, V.J. & Kuprash, D.V. In vitro selection of optimal RelB/p52 DNA-binding motifs. *Biochem Biophys Res Commun* 365, 583-588 (2008).
7. Wang, J. *et al.* Distinct roles of different NF-kappa B subunits in regulating inflammatory and T cell stimulatory gene expression in dendritic cells. *J Immunol* 178, 6777-6788 (2007).

`

8. Fujita, T., Nolan, G.P., Ghosh, S. & Baltimore, D. Independent modes of transcriptional activation by the p50 and p65 subunits of NF-kappa B. *Genes Dev* 6, 775-787 (1992).
9. Leung, T.H., Hoffmann, A. & Baltimore, D. One nucleotide in a kappaB site can determine cofactor specificity for NF-kappaB dimers. *Cell* 118, 453-464 (2004).
10. Bryne, J.C. *et al.* JASPAR, the open access database of transcription factor-binding profiles: new content and tools in the 2008 update. *Nucleic Acids Res* 36, D102-106 (2008).
11. Grilli, M., Chiu, J.J. & Lenardo, M.J. NF-kappa B and Rel: participants in a multiform transcriptional regulatory system. *Int Rev Cytol* 143, 1-62 (1993).
12. Kunsch, C., Ruben, S.M. & Rosen, C.A. Selection of optimal kappa B/Rel DNA-binding motifs: interaction of both subunits of NF-kappa B with DNA is required for transcriptional activation. *Mol Cell Biol* 12, 4412-4421 (1992).
13. Lim, C.A. *et al.* Genome-wide mapping of RELA(p65) binding identifies E2F1 as a transcriptional activator recruited by NF-kappaB upon TLR4 activation. *Mol Cell* 27, 622-635 (2007).
14. Kasowski, M. *et al.* Variation in transcription factor binding among humans. *Science* 328, 232-235 (2010).
15. Schreiber, J. *et al.* Coordinated binding of NF-kappaB family members in the response of human cells to lipopolysaccharide. *Proc Natl Acad Sci U S A* 103, 5899-5904 (2006).

`

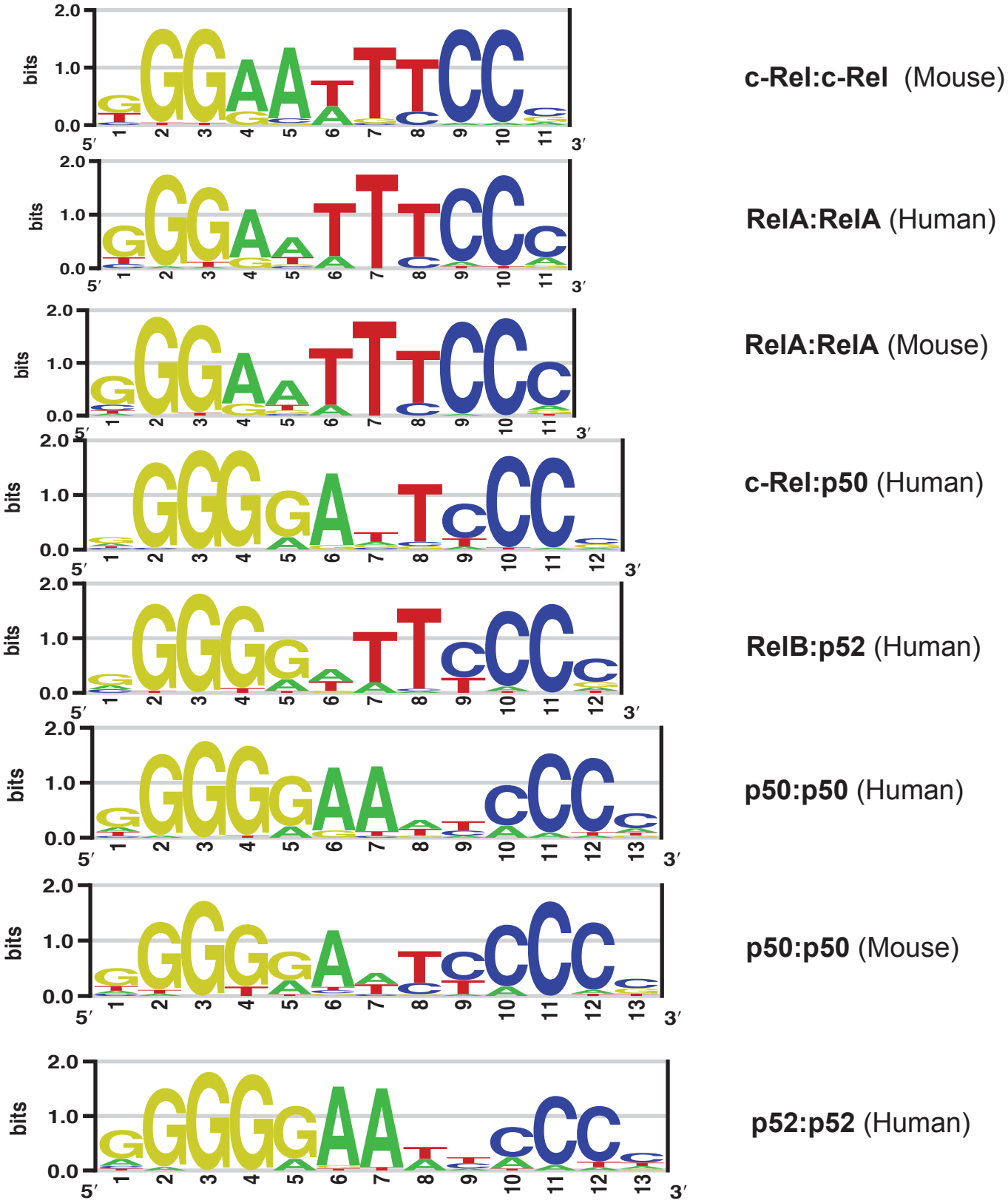

Supplementary Figure 1. DNA binding site motifs derived from Universal PBM (uPBM) experiments performed on eight NF-kB dimers.

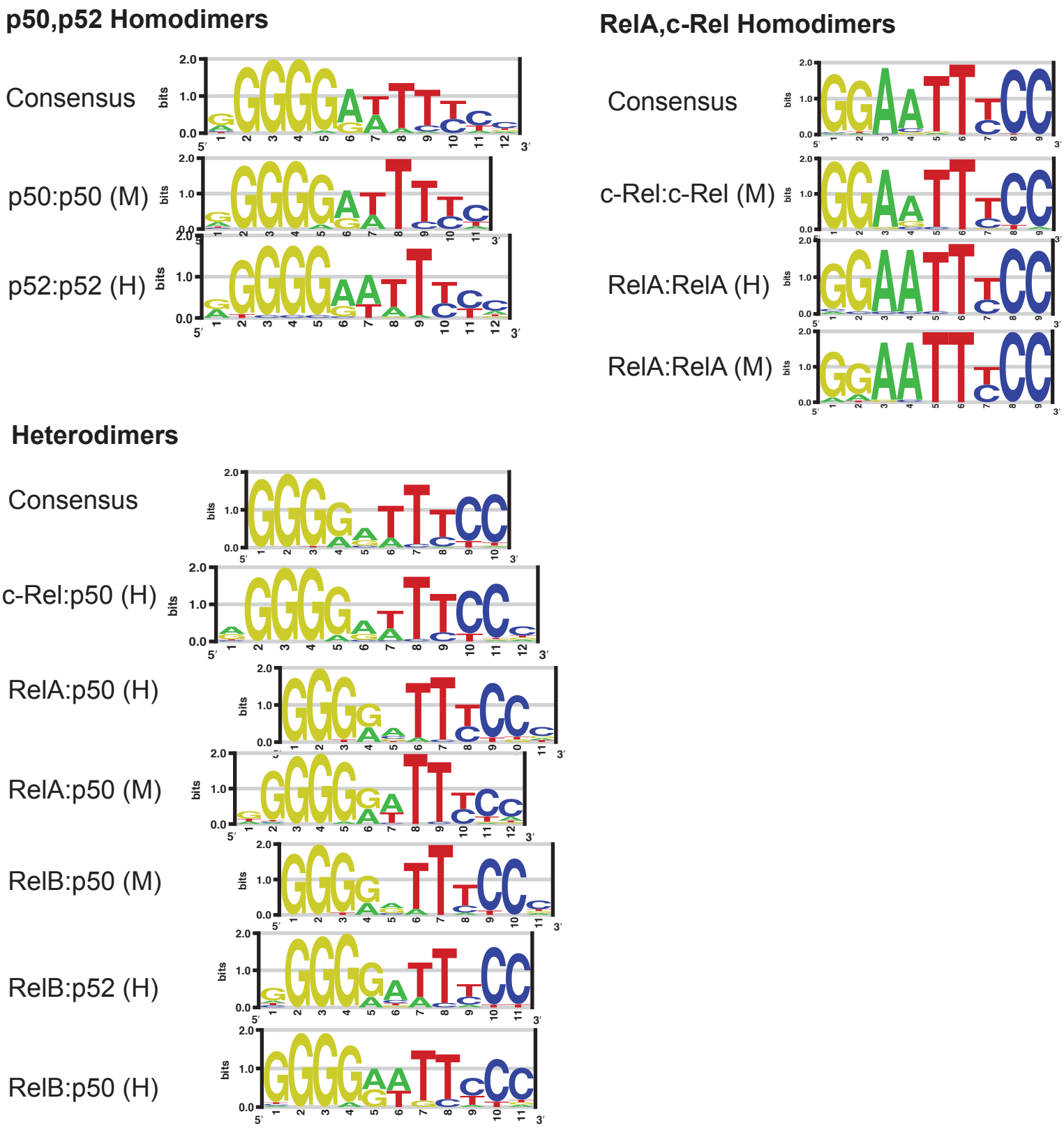

Supplementary Figure 2. DNA binding site motifs derived from top-scoring κB sites from custom NF-κB PBM experiments. DNA binding site motifs determined from the 25 highest scoring κB sites (i.e., κB sites with highest z-scores) identified in our 12 custom NF-κB PBM experiments. Motifs are grouped according to the three NF-κB dimers clusters (**Fig. 1**). A consensus motif determined using the aggregate set of top-scoring κB sites from all cluster members is also shown.

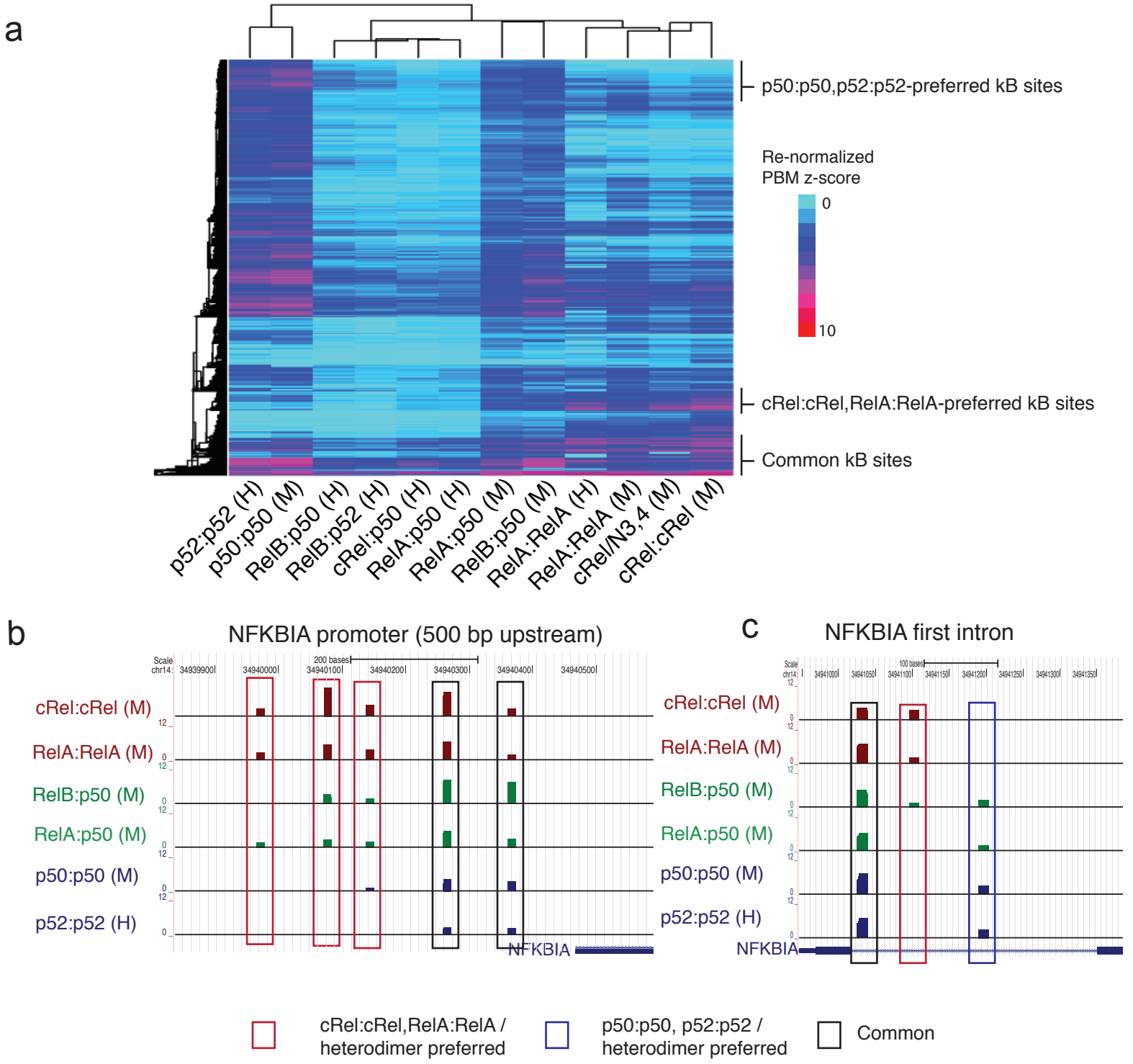

Supplementary Figure 3. Binding landscape for NF-κB dimers. **(a)** Heatmap showing the binding of twelve NF-kB dimers to ~2850 10-bp κB sites. PBM z-scores for each dimer are normazlied 0 to 10 scale. Examples of sequence space regions (i.e. sets κB sequences) preferred by particular dimers are indicated. **(b,c)** Putative κB sites identified for six dimers in the (b) proximal upstream promoter (500 base pairs) and (c) first intron of NFKBIA are shown (human genome, hg18, see Methods). The z-score for each identified κB site is indicated by the height of the bar. Dimers are color coded according to the 3 dimer classes (**Fig. 1**). Sites preferred by particular dimers, as well as those bound well by all dimers, are indicated.

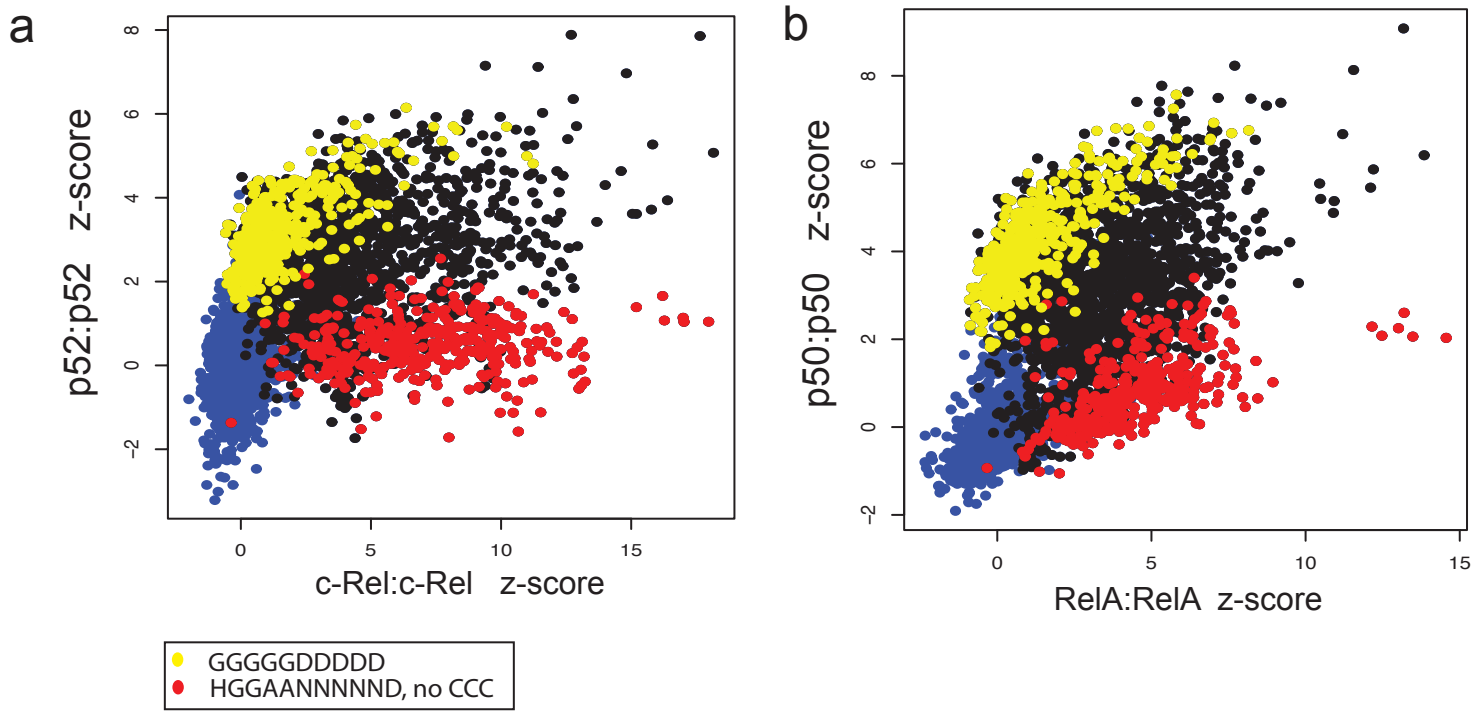

Supplementary Figure 4. Dimer-specific binding to traditional and non-traditional κB. Comparison (as in **Fig. 2**) of NF-κB dimer binding to 3,285 κB sites (black dots) and a background set of 1,200 random 10-mers (blue dots): (**a**) mouse p52:p52 and c-Rel:c-Rel homodimers; (**b**) mouse p50:p50 and RelA:RelA. κB sites conforming to the patterns 5′-GGGGGNNNNN-3′ (N = any base) and 5′-HGGAANNNNND-3′ (H = not G, D = not C, NNNNN = all 5-mers except those containing CCC triplets) are highlighted in yellow and red, respectively.

a

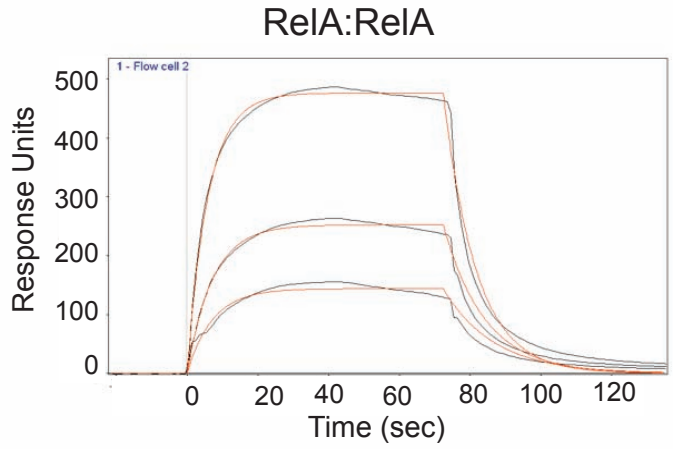

b

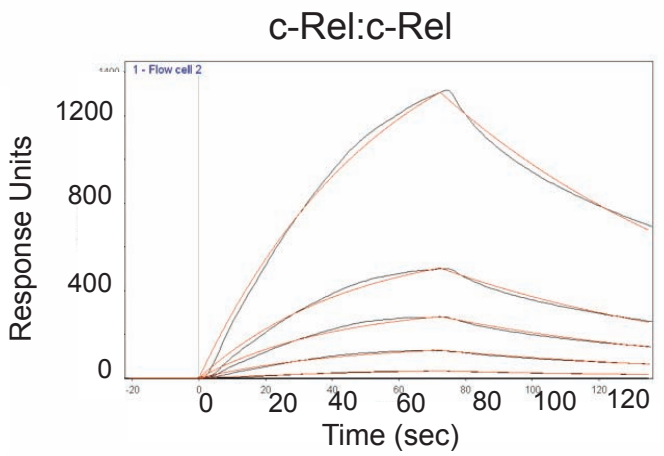

c

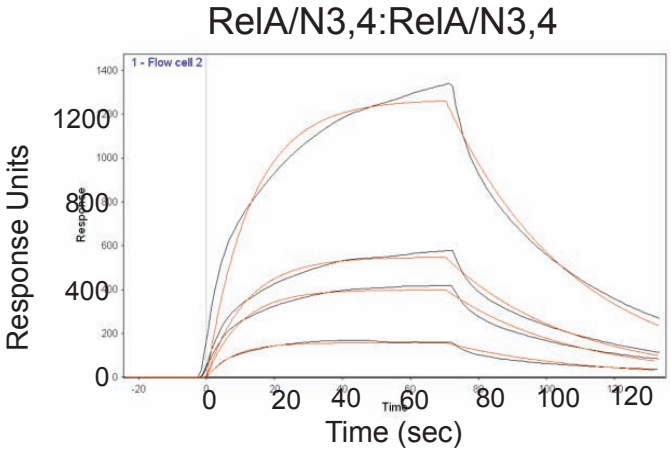

d

	k_{on} ($M^{-1}s^{-1}$)	k_{off} (s^{-1})	Kd (nM)
RelA:RelA	125000 (110000)	0.0977 (0.0186)	1282 (807)
c-Rel:c-Rel	89700 (59000)	0.0108 (0.0003)	207 (166)
RelA/N3,4: RelA/N3,4	579000 (480000)	0.0278 (0.0016)	85 (64)

Supplementary Figure 5. SPR response curves and data fits. Response curves (black line) and data fits are shown for SPR experiments with three NF-κB dimers and the *Il12b* proximal DNA probe. **(a)** SPR data for RelA:RelA homodimer experiment, concentration of protein applied to SPR sensor chip was 211 nM (bottom curve), 351 nM and 702 nM (top curve). **(b)** SPR data for c-Rel:c-Rel homodimer experiment, concentration of protein applied to SPR sensor chip was 35 nM (bottom curve), 71 nM, 118 nM, 155 nM, and 353 nM (top curve). **(c)** SPR data for RelA/N3,4:RelA/N3,4 homodimer experiment, concentration of protein applied to SPR sensor chip was 65 nM (bottom curve), 130 nM, 163 nM, and 325 nM (top curve). **(d)**, K_{on}, K_{off}, and Kd values are shown for each of the three proteins with the IL12b/p40 probe. The values shown represent the means of the computationally determined values for all of the protein concentrations analyzed for each dimer, with standard deviations shown in parenthesis. Standard deviations for the K_{off} values are much smaller than for K_{on} and Kd values. Large standard deviations for K_{on} and Kd values were observed when analyzing all dimers and all DNA sequences, and reflect variability in the K_{on} values calculated for the different protein concentrations.

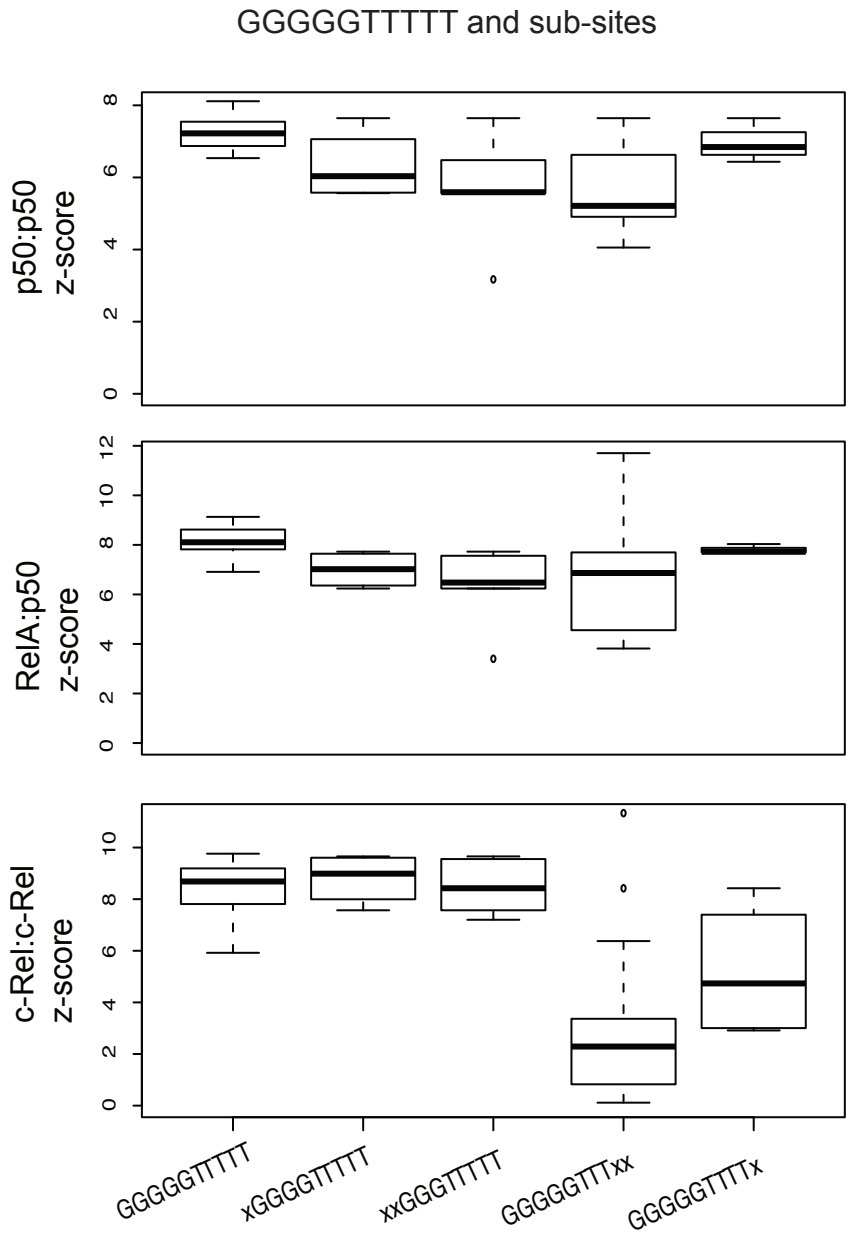

Supplementary Figure 6. Z-score distributions for the non-traditional 10-bp κB site 5′-GGGGGTTTTT-3′ and shorter variant sites (as in **Fig 3**). Score distribution for 10-bp sites are as in (**Fig 3a**). Score distributions for shorter sites are determined by examining scores from all κB sites in our dataset that contained the sub-site sequence. For example, column 2 labeled xGGGGTTTTT has scores from the 4 κB sites where x = A,C,G or T.

Nature Immunology doi:10.1038/ni.2151

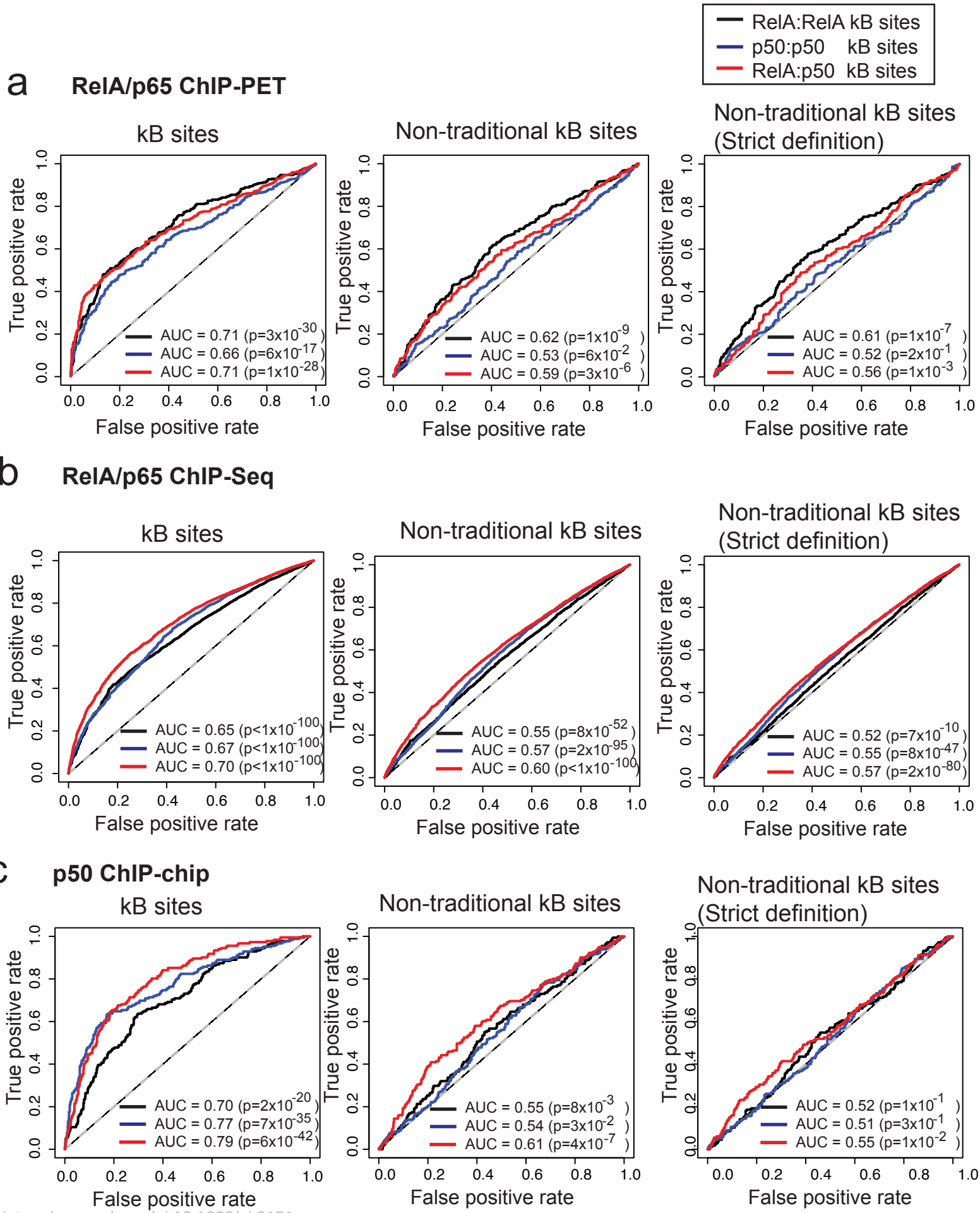
RelA:RelA kB sites
p50:p50 kB sites
RelA:p50 kB sites
a
RelA/p65 ChIP-PET
kB sites
Non-traditional kB sites
Non-traditional kB sites (Strict definition)
True positive rate
False positive rate
AUC = 0.71 (p=3x10-30)
AUC = 0.66 (p=6x10-17)
AUC = 0.71 (p=1x10-28)
AUC = 0.62 (p=1x10-9)
AUC = 0.53 (p=6x10-2)
AUC = 0.59 (p=3x10-6)
AUC = 0.61 (p=1x10-7)
AUC = 0.52 (p=2x10-1)
AUC = 0.56 (p=1x10-3)
b
RelA/p65 ChIP-Seq
kB sites
Non-traditional kB sites
Non-traditional kB sites (Strict definition)
AUC = 0.65 (p<1x10-100)
AUC = 0.67 (p<1x10-100)
AUC = 0.70 (p<1x10-100)
AUC = 0.55 (p=8x10-52)
AUC = 0.57 (p=2x10-95)
AUC = 0.60 (p<1x10-100)
AUC = 0.52 (p=7x10-10)
AUC = 0.55 (p=8x10-47)
AUC = 0.57 (p=2x10-80)
c
p50 ChIP-chip
kB sites
Non-traditional kB sites
Non-traditional kB sites (Strict definition)
AUC = 0.70 (p=2x10-20)
AUC = 0.77 (p=7x10-35)
AUC = 0.79 (p=6x10-42)
AUC = 0.55 (p=8x10-3)
AUC = 0.54 (p=3x10-2)
AUC = 0.61 (p=4x10-7)
AUC = 0.52 (p=1x10-1)
AUC = 0.51 (p=3x10-1)
AUC = 0.55 (p=1x10-2)

Supplementary Figure 7. Enrichment of PBM-determined κB sites in dimer-bound genomic regions. Analyses are shown for three ChIP datasets: **(a)** RelA/p65 binding in lipopolysaccharide (LPS)-stimulated human monocytes[13]; **(b)** RelA/p65 binding in TNFα-stimulated human lymphoblastoid cell lines[14]; **(c)** p50 binding in LPS-stimulated U937 cells[15]. Receiver operating characteristic (ROC) curve analyses quantifying the enrichment within dimer-bound regions of PBM-determined κB sites are shown (see Supplementary Methods). ROC curves are shown for analyses using PBM data from three different NF-kB dimers: RelA:RelA (black line); p50:p50 (blue line); RelA:p50 (red line). For each dataset, analyses were performed using (**left panel**) all kB sites from each PBM experiment; (**middle panel**) non-traditional sites defined with the 1 SD cutoff (i.e., all traditional sites scoring above the 1 SD PWM cutoff were masked out of the genomic regions, see Supplemental Methods); (**right panel**) non-traditional sites defined with the 2 SD cutoff (most strict definition of non-traditional). Area under the ROC curve (AUC) values are reported to quantify the enrichment, and a Wilcox-Mann-Whitney U test was applied to calculate the significance of each AUC value (see Supplemental Methods).

a Scoring a 9-mer with 8-mers and 7-mers

9-mer	**GGGAATTCC**	ln(F)
8-mer	**GGGAATTC**	**+13**
8-mer	GGAATTC**C**	**+11**
7-mer	GGAATTC	**-9**
	GGGAATTCC	**15**

← Subtract 7-mer score so contribution from GGAATTC subsequence is not double counted

F : k-mer median fluorescence intensity from uPBM experiment

b Scoring a 10-mer with 8-mers and 7-mers

10-mer	**GGGAATTCCC**	ln(F)
8-mer	**GGGAATTC**	**+13**
8-mer	GGAATTC**C**	**+11**
7-mer	GGAATTC	**-9**
8-mer	GAATTCC**C**	**+15**
7-mer	GAATTCC	**-10**
	GGGAATTCC	**20**

c Scoring a 10-mer with *gapped* 8-mers and 7-mers

10-mer	**GGGAATTCCC**	ln(F)
8-mer	**GGGA..TCCC**	**+13**
8-mer	GGA**A.**TCCC	**+11**
7-mer	GGA..TCCC	**-9**
8-mer	GGA**.T**TCCC	**+15**
7-mer	GGA..TCCC	**-10**
	GGGAATTCC	**20**

Supplementary Figure 8. Outline of method for scoring k-mers using scores of shorter k-mers obtained by universal PBM experiment. (**a**) Method for scoring a 9-mer using the scores (i.e., natural log of k-mer median intensities) of two constituent 8-mers and a 7-mer. (**b**),(**c**) Method for scoring 10-mers with contiguous or gapped constituent k-mers, respectively. Bases in bold indicate the energy contributions being added at each step.

a

10-mer	**GGGAATTCCC**	ln(F)	1111111111	10-mer
8-mer	**GGGAATTC**	**+13**	+**11111111**	8-mer
8-mer	GGAATTC**C**	**+11**	+ 1111111**1**	8-mer
7-mer	GGAATTC	**-9**	- 1111111	7-mer
8-mer	GAATTCC**C**	**+15**	+ 1111111**1**	8-mer
7-mer	GAATTCC	**-10**	- 1111111	7-mer
	GGGAATTCC	**20**		

b

Scheme 1		Scheme 2		Scheme 3	
#1111111111	10-mer	#1111111111	10-mer	#1111111111	10-mer
+**11111111**	8-mer	+**111.1.1111**	8-mer	+**11.11.111**	8-mer
+ 1111111**1**	8-mer	+111**1**..1111	8-mer	+11**1**.1.1111	8-mer
- 1111111	7-mer	-111...1111	7-mer	-11..1.1111	7-mer
+ 1111111**1**	8-mer	+111.1**1**.111	8-mer	+11.1.**1**1111	8-mer
- 1111111	7-mer	-111.11..11	7-mer	-11.1..1111	7-mer

Supplementary Figure 9. Patterns of k-mers used to score 10-bp κB sites. (**a**) The scoring method for 10-bp κB site 5′-GGGAATTCCC-3′ (left), the pattern scheme used to score the site (right) (**b**) The three scoring schemes used in this work to score 10-bp κB sites, final scores for each 10-bp κB site is an average of the three scores.

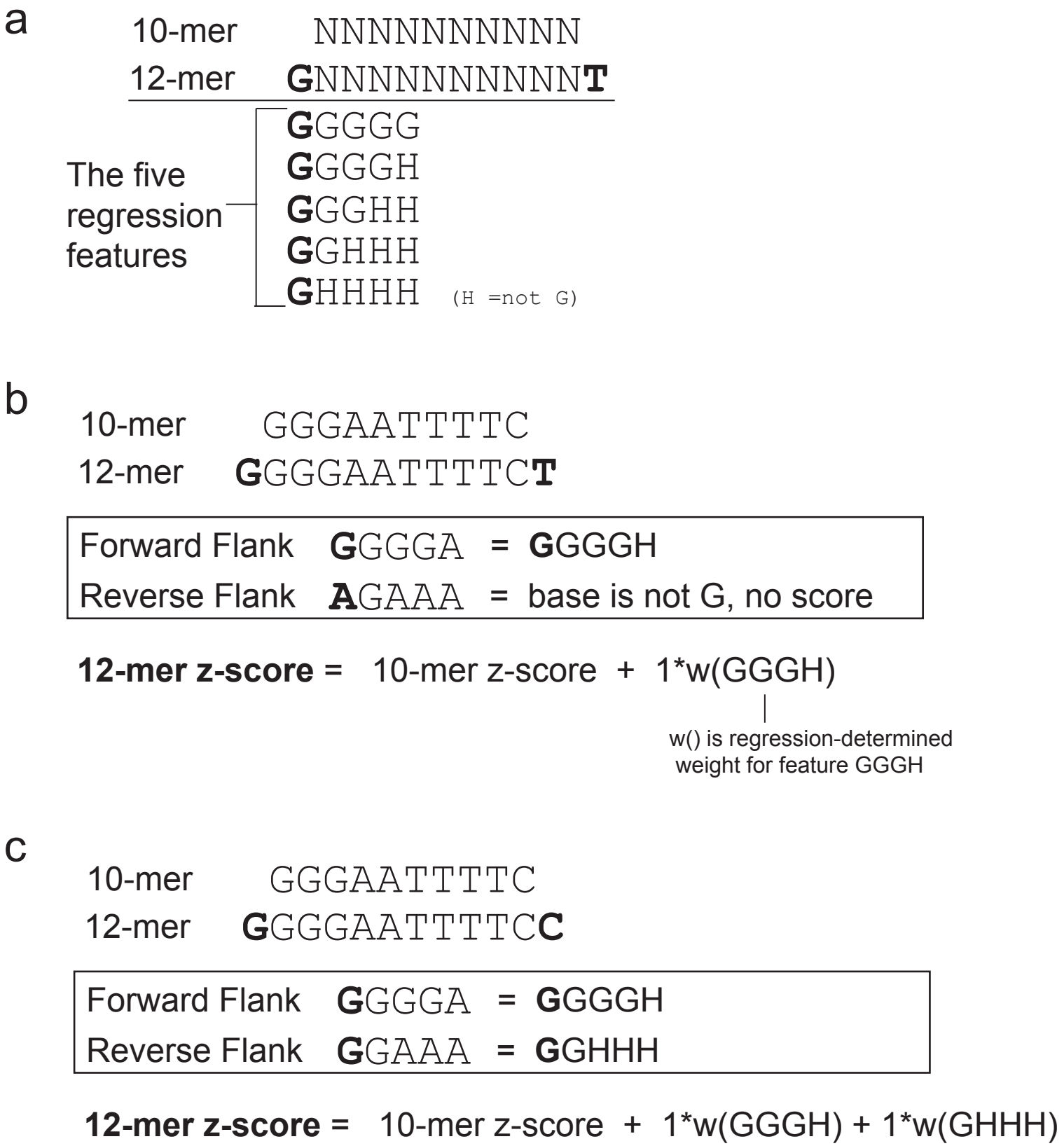

Supplementary Figure 10. Schematic of algorithm for scoring 12-bp κB sites. **(a)** Shown are the five regression features (i.e., patterns of the four bases immediately adjacent to a 5' flanking guanine) used to evaluate the contribution to binding of a 5′ flanking guanine base. Only a single regression feature will describe any particular 5′ flanking guanine. **(b,c)** Examples of the scoring for two different 12-bp κB sites.

Nature Immunology doi:10.1038/ni.2151

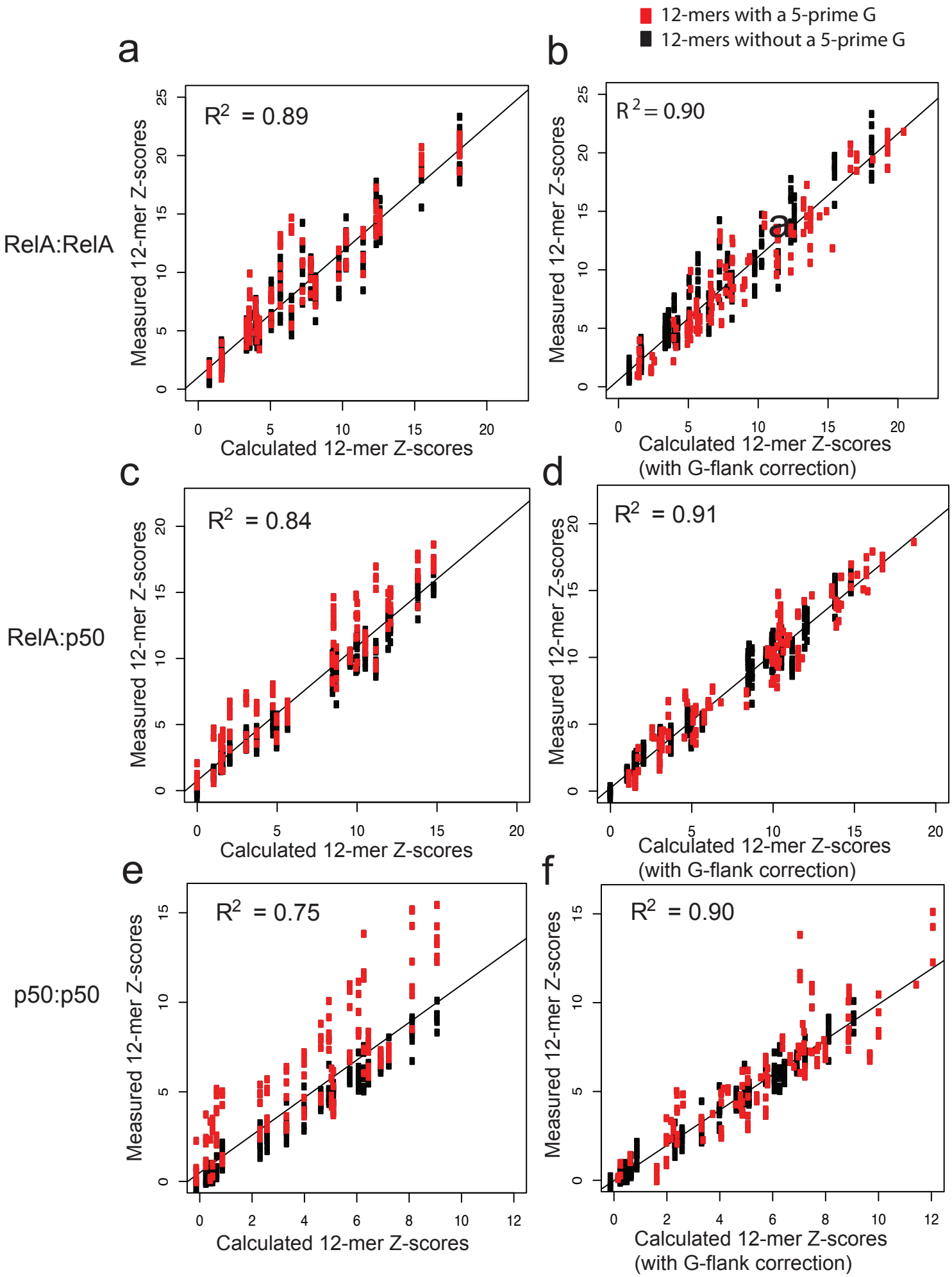

Nature Immunology doi:10.1038/ni.2151

Supplementary Figure 11. Correlation of 352 PBM-measured and calculated 12-bp binding z-scores for three NF-kB dimer PBM experiments. Calculated 12-bp z-scores are calculated with adjustment for guanine flanking bases (b,d and f) and without (a,c, and e). Adjustments for guanine flanks are described in Supplemetnary Methods. Z-scores without guanine-flank adjustments are the z-scores of the central 10-bp site of each 12-bp site. Data points are colored according to the identity of the 5′ flanking bases added to generate each 12-bp site: at least one 5′ flanking base is a guanine base (red), neither 5' flanking base is a guanine (black).

Nature Immunology doi:10.1038/ni.2151

	Sequence	Probe ID	p50:p50 (sec)	c-Rel:c-Rel (sec)	RelA;RelA (sec)	RelA/N3,4:RelA/N3,4 (sec)	RelA:p50 (sec)	c-Rel:p50 (sec)	RelB:p50 (sec)	RelB:p52 (sec)
1	GGAAATTCCC	p65-7	120 (27)	367 (54)	45 (1)	115 (17)	326 (89)	2483 (492)	226 (18)	148 (13)
2	GGGGAATTTT	IL12b/p40	113 (12)	64 (2)	7 (2)	25 (1)	57 (3)	277 (6)	53 (2)	84 (3)
3	GGGGGTTTTT	PBM2	437 (77)	58 (11)	7 (1)	28 (6)	123 (17)	366 (84)	159 (25)	171 (33)
4	GGGGGGAGTA	PBM3	91 (27)	4 (1)	4 (1)	8 (5)	58 (17)	35 (11)	65 (11)	107 (43)
5	GGAATTTCTT	CD28RE	6 (0.2)	92 (10)	3 (1)	39 (2)	13 (2)	70 (10)	27 (14)	49 (19)
6	AGGAATTCCA	PBM1	9 (2)	46 (8)	1 (0.3)	22 (3)	6 (2)	46 (3)	13 (6)	49 (28)

Supplementary Table 1. SPR-determined dissociation half-life values ($t_{1/2}$) for different NF-κB dimers and κB sites. Half-life values, directly proportional to dissociation off-rates ($t_{1/2} = \ln(2)/K_{off}$), are listed for six different 10-bp κB site sequences (Methods, **Fig. 2**), and for eight different mouse NF-κB dimers (Columns 3-6).

Protein	Species	Concentratio	Salt	Primary Ab	Secondary Ab
c-Rel:c-Rel	Mouse	140 nM	80 mM NaCl	cRel (10 μL)	Rabbit IgG (5 μL)
RelA:RelA	Human	170 nM	80 mM NaCl	p65 (10 μL)	Rabbit IgG (5 μL)
RelA:RelA	Mouse	120 nM	80 mM NaCl	p65 (10 μL)	Rabbit IgG (5 μL)
RelA/N3,4	Mouse	180 nM	80 mM NaCl	p65 (10 μL)	Rabbit IgG (5 μL)
c-Rel:p50	Human	160 nM	50 mM NaCl	p65 (10 μL)	Rabbit IgG (5 μL)
RelA:p50	Human	160 nM	50 mM NaCl	p65 (10 μL)	Rabbit IgG (5 μL)
RelA:p50	Mouse	160 nM	50 mM NaCl	p65 (10 μL)	Rabbit IgG (5 μL)
RelB:p50	Mouse	170 nM	50 mM NaCl	p65 (10 μL)	Rabbit IgG (5 μL)
RelB:p52	Human	170 nM	50 mM NaCl	His-tag (20 μL)	Rabbit IgG (5 μL)
RelB:p50	Human	180 nM	50 mM NaCl	His-tag (20 μL)	Rabbit IgG (5 μL)
p50:p50	Mouse	200 nM	50 mM NaCl	p50 (10 μL)	Rabbit IgG (5 μL)
p52:p52	Human	200 nM	50 mM NaCl	His-tag (20 μL)	Rabbit IgG (5 μL)

Epitopes	Antibody
His-tag	Alexa Fluor 488 conjugated Penta-His, 200 μg/ml (Qiagen, Cat# 35310)
p50	NF-κB p50 rabbit polyclonal IgG, 200 μg/ml (Santa Cruz, Cat# sc-114)
c-Rel	c-Rel (N) rabbit polyclonal IgG, 200 μg/ml (Santa Cruz, Cat# 70)
p65	NF-kB p65 (A) rabbit polyclonal IgG, 200 μg/ml (Santa Cruz, Cat# sc-109)
Rabbit IgG	Alexa Fluor 488 goat anit-rabbit IgG , 2 mg/ml (Invitrogen, Cat# A11034)

Supplementary Table 2. Universal PBM (UPBM) experiment details. (**a**) Concentration (column 2) indicates the final concentration of the protein in the PBM binding reaction. Salt (column 3) indicates the salt identity and final concentration in the PBM binding reaction. Primary and Secondary Ab (columns 3 and 4) indicate the epitope and amount of antibody (per 200 μl) used to label the PBM-bound protein; details for each antibody are listed at the bottom. Some of the PBM experiments did not require a secondary Alexa488-conjugated antibody as the primary Penta-His antibody was Alexa488-labelled.

Protein	Species	Concentration	Salt	Primary Ab	Secondary Ab
p50:p50 (exp #1)	Human	430 nM	80 mM NaCl	His-tag (20 μL)	n/a
p50:p50 (exp #2)	Human	430 nM	80 mM NaCl	p50 (20 μL)	Rabbit IgG (20 μL)
p50:p50	Mouse	280 nM	50 mM NaCl	p50 (20 μL)	Rabbit IgG (5 μL)
p52:p52	Human	500 nM	80 mM NaCl	His-tag (20 μL)	n/a
c-Rel:c-Rel	Mouse	280 nM	50 mM NaCl	cRel (20 μL)	Rabbit IgG (5 μL)
RelA:RelA	Human	280 nM	80 mM KCl	His-tag (20 μL)	n/a
RelA:RelA	Mouse	280 nM	80 mM NaCl	RelA/p65 (20 μL)	Rabbit IgG (5 μL)
c-Rel:p50	Human	210 nM	50 mM NaCl	His-tag (20 μL)	n/a
RelB:p52	Human	188 nM	50 mM NaCl	His-tag (20 μL)	n/a

Epitopes	Antibody
His-tag	Alexa Fluor 488 conjugated Penta-His, 200 μg/ml (Qiagen, Cat# 35310)
p50	NF-κB p50 rabbit polyclonal IgG, 200 μg/ml (Santa Cruz, Cat# sc-114)
c-Rel	c-Rel (N) rabbit polyclonal IgG, 200 μg/ml (Santa Cruz, Cat# 70)
p65	NF-kB p65 (A) rabbit polyclonal IgG, 200 μg/ml (Santa Cruz, Cat# sc-109)
Rabbit IgG	Alexa Fluor 488 goat anit-rabbit IgG , 2 mg/ml (Invitrogen, Cat# A11034)

Supplementary Table 3. Custom NF-κB PBM experiment details. (a) Listed are details of the custom NF-κB PBM experiments performed in this study. Columns are as in Supplementary Table 2.